RADIATION EFFECT ON MHD CASSON FLUID FLOW BETWEEN PARALLEL PLATES OF DIFFERENT PERMEABILITY

NITYANAND P. PAI, DEVAKI B., PAREEKSHITH, SAMPATH KUMAR V. S.*, AND VASANTH K. R.

ABSTRACT. This paper intends to analyse the impact of thermal radiation on the Casson fluid flow between uniformly porous parallel plates of different permeability in the presence of the magnetic field using a semi-analytical approach. The fundamental equations of fluid flow are reduced into non-linear ODEs with boundary conditions using similarity transformation and solved using Homotopy Perturbation Method (HPM). The velocity profile and temporal distribution curve for distinct values of M, Rd, Pr, R_i, Ec, and β are displayed in the figures. The impacts of these physical parameters on coefficient of skin friction and heat transfer rate are also analysed using HPM. It is observed that for the mixed suction, rise in radiation impact suppresses the thermal border thickness, resulting decrement in the temporal distribution, whereas an opposite trend is observed for mixed injection case. Further, this research provides valuable insights for industries working with nuclear reactors and magnetic material transmissions.

1. Introduction

Magnetohydrodynamics (MHD), is one of the most interesting and challenging fields in fluid flows. The concept of MHD, along with the radiation impact, has extensive applications in nuclear fusion reactors, electromagnetic pumps and generators, metallurgy, oil and gas industries, the study of plasma, and many more. Due to its broad scope in engineering and technological problems, MHD and radiation impact on the fluid flow through a media of different permeability has received good responses from the researchers. Permeability is one of the most critical parameters to study and characterise permeable channels. The term "permeability" pertains to the inherent ability of a given material to allow the passage or flow of fluid particles through it, indicating the degree of porosity of the material's structure. This property is often measured and quantified in terms of the rate at which a particular fluid can permeate the material under specific conditions. The concept of permeability plays a vital role in various fields, such as engineering, geology, chemistry, etc. The permeability of a material is determined by the structure and composition along with the properties of the fluid passing through

it. In general, materials that are more porous or have larger spaces between their particles tend to have higher permeability. Understanding the concept of permeability is crucial for designing and evaluating systems that involve fluid flow, such as oil wells, water filtration systems, and underground aquifers. Moreover, the applications also depend on the fluid under consideration.

A class of non-Newtonian fluids known as Casson fluids has a wide range of applications in food industries to thicken and stabilize food products, in petroleum industries to enhance oil recovery, in pharmaceutical industries for drug delivery systems, the medical field for blood flow stimulation and study cerebral spinal fluid dynamics. A. S. Berman [3] initiated the investigation of a two-dimensional laminar flow of a Newtonian fluid through a uniformly porous channel. J. R. Sellars [22] and R. M. Terrill [25] extended this work to obtain solutions for small and large Reynolds numbers. Further, S. W. Yuan [27] studied for large negative Reynolds numbers. R. M. Terrill and G. M. Shrestha [26] extended the study of laminar flow through uniformly porous channels to plates of different permeability and obtained the solution numerically. Further, N. M. Bujurke et al. [5] extended the concept to obtain the solution using long series analysis. Several other researchers have also contributed to the study of flows in porous media [9, 19].

Heat transmission in an MHD fluid between two insulated parallel infinite plates was investigated by H. A. Attia and N. A. Kotb [1]. S. Ganesh and S. Krishnambal [6] studied the impact of MHD on the flow of a viscous fluid between two parallel plates and obtained a solution for smaller values of Reynolds number using a numerical method. Sampath Kumar V.S. et al. [21] investigated the MHD impact on the flow between two plates, of which the bottom plate is porous with injection and suction impact. Many more researchers have contributed to the study of MHD flow in recent years [10, 7].

A. Raptis [16] studied the impact of radiation on a two-dimensional steady free convection flow between two infinite porous plates. H. Sithole et al. [23] numerically simulated the flow of couple stress nano-fluid through a porous media in the presence of a magnetic field to analyse the impacts of chemical reaction and thermal radiation. Further, N. B. Naduvinamani and U. Shankar [15] investigated the MHD and radiative impacts on the unsteady squeezing flow of a Casson fluid between two parallel plates. Several other researchers have examined the impact of radiation on different models [13, 14, 10, 24].

Due to non-linearity in the models, the solution using known analytical techniques is impossible. However, numerical methods with certain limitations obtain an approximate solution to such a class of problems. To overcome the difficulties encountered in numerical methods, a new class of techniques known as semi-analytical methods was brought into the picture. HPM was first proposed by J. H. He [11, 12] in 1998. Further, numerous researchers have also utilized HPM to resolve various wave-like, differential, and integral equations [4, 2, 17, 8].

The current article intends to employ a semi-analytical method, specifically HPM, to analyse the combined impacts of radiation and MHD on the flow of Casson fluid between two parallel plates of different permeability. Accurate results are obtained using the method for this geometry. Also, the method has advantages in comparison to other mathematical techniques. Further, it is crucial to note that

a single computer program is capable of yielding solutions for a large expansions rather than a single term. Additionally, the method is so stable that it reveals the analytic structure of the solution function [18, 20]. It is evident that HPM is capable of yielding results with a negligible amount of labour in computation.

2. Mathematical Formulation

Let two uniformly porous plates of different permeability be placed at a distance h apart. Consider a two-dimensional flow of an incompressible MHD Casson fluid with the impact of radiation in a channel with the velocity vector q between the plates as in Figure (1). The Reynolds number $R_i = (V_i h)/\nu$ for $|V_i| \geq |V_j|$, where ν is the kinematic viscosity.
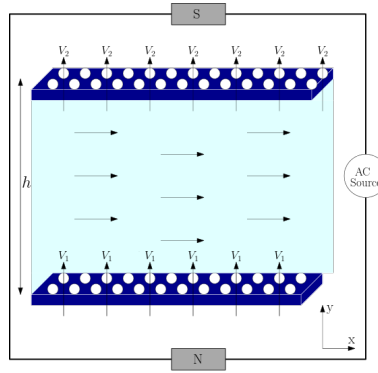

FIGURE 1. Geometry of the flow

The fluid flow equations for a steady incompressible laminar flow are given by

$$\nabla . q = 0 \tag{2.1}$$

$$(q.\nabla)q = -\frac{\nabla . P}{\rho} + \nu \left(1 + \frac{1}{\beta}\right)\nabla^2 . q - \frac{\sigma}{\rho}B_0^2 u \tag{2.2}$$

$$q.(\nabla T) = \frac{1}{\rho C_P}\left(k_0\nabla^2 T - \nabla . q_{rad} + \mu \left(1 + \frac{1}{\beta}\right)(\nabla \times q)^2\right). \tag{2.3}$$

In the above set of equations, u and v are the velocity components along x and y directions respectively. The density and coefficient of viscosity of the fluid are denoted respectively by ρ and μ. The notations σ and B_0 are used to represent the fluid electrical conductivity and applied magnetic field on the system. The temperature of the system, thermal conductivity and specific heat of the fluid are respectively denoted by T, k_0 and C_P. An expression for radiative heat flux, q_{rad}, is obtained by Rosseland's approximation as

$$q_{rad} = \frac{4\sigma^*}{3k^*}\frac{\partial T^4}{\partial y}. \tag{2.4}$$

By Taylor's series about T_1,

$$T^4 \cong 4T_1^3 T - 3T_1^4.$$

Let η given by $\eta = \dfrac{y}{h}$, be a non-dimensional variable introduced in (2.1) - (2.3).

Let V_1 and V_2 be the constant velocities at which the fluid is sucked or injected for a two dimensional flow at the bottom and top plates respectively. The boundary conditions are

$$v(x,0) = V_1, \qquad v(x,h) = V_2 \tag{2.5}$$

$$u(x,0) = 0, \qquad u(x,h) = 0 \tag{2.6}$$

$$T = \begin{cases} T_1 & \text{for} \quad \eta = 0 \\ T_2 & \text{for} \quad \eta = 1. \end{cases} \tag{2.7}$$

Two different cases arise in solving this problem, that is $|V_2| \geq |V_1|$ and $|V_1| \geq |V_2|$. The problem to be solved in the case of suction and injection for $|V_2| \geq |V_1|$ can be reduced to problem for $|V_1| \geq |V_2|$. Whereas in case of mixed flow, both $|V_2| \geq |V_1|$ and $|V_1| \geq |V_2|$ are to be solved separately. Berman [3] assumed the existence of stream function for a two dimensional incompressible flow is as follows

$$\Psi(x,\eta) = \left[\frac{hU(0)}{a_i} - V_i x \right] F(\eta). \tag{2.8}$$

Let $a_i = (-1)^i \left(1 - \dfrac{V_j}{V_i} \right)$ for $i, j \in \{1, 2\}$, such that

$$u(x,\eta) = \left(\frac{1}{h} \right) \left(\frac{\partial \Psi}{\partial \eta} \right) \tag{2.9}$$

$$v(x,\eta) = -\left(\frac{\partial \Psi}{\partial x} \right), \tag{2.10}$$

satisfy the continuity equation (2.1). Hence,

$$u(x,\eta) = \left[\frac{U(0)}{a_i} - \frac{V_i x}{h} \right] \frac{dF}{d\eta} \tag{2.11}$$

$$v(\eta) = V_i F(\eta). \tag{2.12}$$

The scalar equation is obtained by substituting the stream function and velocity in (2.2).

$$\left(1 + \frac{1}{\beta} \right) \frac{dF^4}{d^4\eta} - R_i \left[F \frac{dF^3}{d^3\eta} - \frac{dF}{d\eta} \frac{dF^2}{d^2\eta} \right] - M^2 \frac{dF^2}{d^2\eta} = 0, \tag{2.13}$$

with boundary conditions,

(1) For $|V_2| \geq |V_1|$

$$F(0) = 1 - a_2, \qquad F(1) = 1 \tag{2.14}$$

$$\frac{dF(0)}{d\eta} = 0, \qquad \frac{dF(1)}{d\eta} = 0. \tag{2.15}$$

(2) For $|V_1| \geq |V_2|$

$$\frac{dF(0)}{d\eta} = 0, \quad \frac{dF(1)}{d\eta} = 0 \qquad (2.16)$$

$$F(0) = 1, \quad F(1) = 1 + a_1. \qquad (2.17)$$

The boundary conditions (2.14) - (2.17) imply that for the case of suction $-2 \leq a_1 \leq -1$ and $1 \leq a_2 \leq 2$, whereas in the mixed case $-1 \leq a_1 \leq 0$ and $0 \leq a_2 \leq 1$.

By using the transformation

$$\theta = \frac{T - T_1}{T_2 - T_1}, \qquad (2.18)$$

the energy equation is transformed into

$$\left(1 + \frac{4}{3}Rd\right)\frac{d\theta^2}{d^2\eta} - R_i Pr F \frac{d\theta}{d\eta} + PrEc\left(1 + \frac{1}{\beta}\right)\left(\frac{dF^2}{d^2\eta}\right)^2 = 0, \qquad (2.19)$$

with boundary conditions

$$\theta(1) = 1, \quad \theta(0) = 0. \qquad (2.20)$$

Where Rd is the radiation parameter, M magnetic parameter, Ec Eckert number and Pr Prandtl number are defined as below:

$$M = B_0 h \sqrt{\frac{\sigma}{\mu}}, \qquad\qquad\qquad Pr = \frac{C_P \mu}{k_0},$$

$$Ec = \frac{1}{C_P(T_2 - T_1)}\left[\frac{U(0)}{a_i} - \frac{V_i x}{h}\right]^2, \qquad Rd = \frac{4\sigma^* T_1^3}{k_0 k^*}.$$

As the obtained differential equations (2.13 and 2.19) with boundary conditions (2.14 - 2.17 and 2.20) are non-linear, the exact solution cannot be obtained by the known methods, however approximate solutions are obtained through numerical methods. To over come the difficulties involved in numerical methods and to obtain a more approximate solution, researchers came up with the idea of semi-analytical methods. The considered model is approached with HPM and an approximate analytic solution obtained by this method is presented here.

3. Method of solution

The considered problem is solved using HPM [11]. Generally in HPM, a non-linear differential equation is expressed in terms of sum of linear and non-linear terms. Further, by using the concept of homotopy in topological spaces, one can construct a homopoty equation. Assuming the solution of the homotopy equation in terms of power series and comparing the coefficients of different powers of the parameter, and solving the obtained set of differential equations, a set of solution is obtained as prescribed in the perturbation methodology.

In the considered problem, two non-linear differential equations of different orders are obtained. Hence, HPM for system of equations employed is to analyse this model is as follows:

Let A_1 and A_2 be the differential operators operated on an unknown function, $f(\eta)$. Let $f_1(\eta)$ and $f_2(\eta)$ be the two known functions in the equation. Then the considered problem can be expressed as

$$A_i[f(\eta)] - f_i(\eta) = 0. \tag{3.1}$$

Generally, in HPM, A_i can be expressed as

$$A_i = L_i + R_i, \tag{3.2}$$

where L_i denotes the linear parts and the remaining part of the differential operators are given by R_i.

The homotopy equation for (3.1) can be constructed with a wise choice of L_i from the governing equations in the following manner

$$H_i(\xi_i, p) = (1-p)[L_i(\xi_i, p) - L_i(v_0(\eta))] + p[A_i(\xi_i, p) - f_i(\xi)] = 0, \tag{3.3}$$

where v_0 is the initial guess to (3.1) and $i = 1, 2$.

Assuming,

$$\xi_i(\eta, p) = \sum_{n=0}^{\infty} p^n f_n(\eta). \tag{3.4}$$

For $p = 1$, (3.4) is the solution to the considered problem.

The zeroth, first and second order solutions obtained by solving the equation using the above mentioned scheme are as given below:

For mixed injection:

$$F_0 = 1 + 3a_1\eta^2 - 2a_1\eta^3. \tag{3.5}$$

$$
\begin{aligned}
F_1 = \frac{1}{140(1+\beta)}[&7a_1 M^2\eta^2\beta - 70a_1 R_1\eta^2\beta - 32a_1^2 R_1\eta^2\beta - 28a_1 M^2\eta^3\beta \\
&+ 140a_1 R_1\eta^3\beta + 54a_1^2 R_1\eta^3\beta + 35a_1 M^2\eta^4\beta - 70a_1 R_1\eta^4\beta \\
&- 14a_1 M^2\eta^5\beta - 42a_1^2 R_1\eta^5\beta + 28a_1^2 R_1\eta^6\beta - 8a_1 R_1\eta^7\beta].
\end{aligned}
\tag{3.6}
$$

$$
\begin{aligned}
F_2 = \frac{-1}{646800(1+\beta)^2}&a_1(-1+\eta)^2\eta^2(77M^4(3+4\eta-30\eta^2+20\eta^3) \\
&+ 154M^2 R_1(35(-1-4\eta+4\eta^2)+a_1(-25-41\eta+23\eta^2+48\eta^3-25\eta^4+10\eta^5)) \\
&+ R_1^2(32340(-1+2\eta)+770a_1(-18+56\eta+49\eta^2-42\eta^3+21\eta^4) \\
&+ a_1^2(761+7380\eta+13999\eta^2-8950\eta^3+2905\eta^4+504\eta^5+1568\eta^6-448\eta^7)))\beta^2.
\end{aligned}
\tag{3.7}
$$

$$\theta_0 = \eta. \tag{3.8}$$

$$
\begin{aligned}
\theta_1 = \frac{3Pr}{20(3+4Rd)\beta}[&-120a_1^2 Ec\eta - 120a_1^2 Ec\beta\eta + 10R_1\beta\eta + 3a_1 R_1\beta\eta \\
&+ 360a_1^2 Ec\eta^2 + 360a_1^2 Ec\beta\eta^2 - 10R_1\beta\eta^2 - 480a_1^2 2Ec\eta^3 - 480a_1^2 Ec\beta\eta^3 \\
&+ 240a_1^2 Ec\eta^4 + 240a_1^2 Ec\beta\beta^4 - 5a_1 R_1\beta\eta^4 + 2a_1 R_1\beta\eta^5].
\end{aligned}
\tag{3.9}
$$

$$\theta_2 = \frac{1}{8400(3+4Rd)^2\beta(1+\beta)}\big[-45360a_1^2EcPr^2R_1\eta + 3240a1^3EcPr^2R_1\eta$$

$$-60480a_1^2EcPrR_1\beta\eta - 30240a1^3EcPrR_1\beta\eta - 90720a_1^2EcPr^2R_1\beta\eta$$

$$+6480a1^3EcPr^2R_1\beta\eta + 6300Pr^2R_1^2\beta\eta + 2520a1Pr^2R_1^2\beta\eta - 24a_1^2Pr^2R_1^2\beta\eta$$

$$-80640a_1^2EcPrR_1Rd\beta\eta - 40320a1^3EcPrR_1Rd\beta\eta - 60480a_1^2EcPrR_1\beta^2\eta$$

$$-30240a_1^3EcPrR_1\beta^2\eta - 9a1M^2PrR_1\beta^2\eta - 45360a_1^2EcPr^2R_1\beta^2\eta$$

$$+3240a_1^3EcPr^2R_1\beta^2\eta + 630a_1PrR_1^2\beta^2\eta + 312a_1^2PrR_1^2\beta^2\eta + 6300Pr^2R_1^2\beta^2\eta$$

$$+2520a_1Pr^2R_1^2\beta^2\eta - 24a_1^2Pr^2R_1^2\beta^2\eta - 80640a_1^2EcPrR_1Rd\beta^2\eta$$

$$-40320a_1^3EcPrR_1Rd\beta^2\eta - 12a_1M^2PrR_1Rd\beta^2\eta + 840a_1PrR_1^2Rd\beta^2\eta$$

$$+416a_1^2PrR_1^2Rd\beta^2\eta + 226800a_1^2EcPr^2R_1\eta^2 - 45360a_1^2EcM^2Pr\beta\eta$$

$$+453600a_1^2EcPrR_1\beta\eta^2 + 207360a_1^3EcPrR_1\beta\eta + 453600a_1^2EcPr^2R_1\beta\eta^2$$

$$-18900Pr^2R_1^2\beta\eta^2 - 5670a_1Pr^2R_1^2\beta\eta^2 - 604800a_1^2EcM^2PrRd\beta\eta^2$$

$$+604800a_1^2EcPrR_1Rd\beta\eta^2 + 276480a_1^2EcPrR_1Rd\beta\eta^2 - 45360a_1^2EcM^2Pr\beta^2\eta^2$$

$$+453600a_1^2EcPr^2R_1\beta^2\eta^2 + 207360a_1^3EcPrR_1\beta^2\eta^2 + ...\big].$$

$$(3.10)$$

For mixed suction:

$$F_0 = 1 - a_2(-1+\eta)^2(1+2\eta). \tag{3.11}$$

$$F_1 = \frac{-1}{140(1+\beta)}a_2(-1+\eta)^2\eta^2(7M^2(-1+2\eta) \tag{3.12}$$
$$+ 2R_2(35 + a_2(-19 + 5\eta - 6\eta^2 + 4\eta^3)))\beta.$$

$$F_2 = \frac{-1}{646800(1+\beta)^2}a_2(-1+\eta)^2\eta a^2(77M^4(3+4\eta-30\eta^2+20\eta^3) \tag{3.13}$$

$$+154M^2R_2(-1-4\eta+4\eta^2) + a_2(10+99\eta-117\eta^2+48\eta^3-25\eta^4+10\eta^5)$$

$$+ R_2^2(32340(-1+2\eta) + 770a_2(66-112\eta+49\eta^2-42\eta^3+21\eta^4)$$

$$+a_2^2(-17719+28940\eta-23731\eta^2+23390\eta^3-13265\eta^4+504\eta^5+1568\eta^6-448\eta^7)))\beta^2.$$

$$\theta_0 = \eta. \tag{3.14}$$

$$\theta_1 = \frac{3Pr}{20(3+4Rd)\beta}\big[-120a_2^2Ec\eta - 120a_2^2Ec\eta + 10R_2\beta\eta - 7a_2R_2\beta\eta$$

$$+360a_2^2Ec\eta^2 + 360a_2^2Ec\beta\eta^2 - 10R_2\beta\eta^2 + 10a_2R_2\beta\eta^2 - 480a_2^2Ec\eta^3$$

$$-480a_2^2Ec\beta\eta^3 + 240a_2^2Ec\eta^4 + 240a_2^2Ec\beta\eta^4 - 5a_2R_2\beta\eta^4 + 2a_2R_2\beta\eta^5\big].$$

$$(3.15)$$

$$\theta_2 = \frac{1}{8400(3+4Rd)^2\beta(1+\beta)}[-45360a_2^2EcPr^2R_2\eta + 48600a_2^3EcPr^2R_2\eta$$
$$-60480a_2^2EcPrR_2\beta\eta + 30240a_2^3EcPrR_2\beta\eta - 90720a_2^2EcPr^2R_2\beta\eta$$
$$+97200a_2^3EcPr^2R_2\beta\eta + 6300Pr^2R_2^2\beta\eta - 10080a_2Pr^2R_2^2\beta\eta + 3756a_2^2Pr^2R_2^2\beta\eta$$
$$-80640a_2^2EcPrR_2Rd\beta\eta + 40320a_2^3EcPrR_2Rd\beta\eta - 60480a_2^2EcPrR_2\beta^2\eta$$
$$+30240a_2^3EcPrR_2\beta^2\eta - 9a_2M^2PrR_2\beta^2\eta - 45360a_2^2EcPr^2R_2\beta^2\eta$$
$$+48600a_2^3EcPr^2R_2\beta^2\eta + 630a_2PrR_2^2\beta^2\eta - 318a_2^2PrR_2^2\beta^2\eta + 6300Pr^2R_2^2\beta^3\eta$$
$$-10080a_2Pr^2R_2^2\beta^2\eta + 3756a_2^2Pr^2R_2^2\beta^2\eta - 80640a_2^2EcPrR_2Rd\beta^2\eta$$
$$+40320a_2^3EcPrR_2Rd\beta^2\eta - 12a_2M^2PrR_2Rd\beta^2\eta + 840a_2PrR_2^2Rd\beta^2\eta$$
$$-424a_2^2PrR_2^2Rd\beta^2\eta + 226800a_2^2EcPr^2R_2\eta^2 - 226800a_2^3EcPr^2R_2\eta^2$$
$$-45360a_2^2EcM^2Pr\beta\eta^2 + 453600a_2^2EcPrR_2\beta\eta^2 - 246240a_2^3EcPrR_2\beta\eta^2$$
$$+453600a_2^2EcPr^2R_2\beta\eta^2 - 453600a_2^3EcPr^2R_2\beta\eta^2 - 18900Pr^2R_2^2\beta\eta^2$$
$$+32130a_2Pr^2R_2^2\beta\eta^2 - 13230a_2^2Pr^2R_2^2\beta\eta^2 - 60480a_2^2EcM^2PrRd\beta\eta^2$$
$$+604800a_2^2EcPrR_2Rd\beta\eta^2 - 328320a_2^3EcPrR_2Rd\beta\eta^2$$
$$-45360a_2^2EcM^2Pr\beta^2\eta^2 + 453600a_2^2EcPrR_2\beta^2\eta^2 + ...].$$

(3.16)

4. Results and Discussion

In this study, the influence of MHD and thermal radiation on the flow of Casson fluid between parallel plates with different permeability is analysed. By employing HPM, the velocity field, and temporal distribution for distinct ranges of the physical parameter are studied and presented in Figure (2) - Figure (19). Figures (2 - 4) graphically represent the impact of R_2, M and β on the velocity profile for the case of mixed suction and Figure (5 - 7) for mixed injection case. Figures (8 - 13) represent graphically the impact of various parameters on the temporal curve for the case of mixed suction, whereas Figures (14 - 19) in mixed injection case. Tables (1 and 2) display respectively the numerical values of coefficient of skin friction and heat transfer rate on the plates, $F''(0)$ and $\theta'(0)$ representing the coefficients skin friction and rate of heat transfer at the bottom plate and $F''(1)$ and $\theta'(1)$ at the top plate respectively.

Figure (2) illustrates the influence of R_2 on the flow velocity for the case of mixed suction. It is clear that, as R_2 increases, the $F'(\eta)$ increases in the range $0 \le \eta \le 0.5$ and further decreases in the other half. Whereas, a reverse trend is observed in the case of mixed injection, as shown in Figure (5). Figure (3) displays the impact of M on $F'(\eta)$ for $|V_2| \ge |V_1|$. It is observed that $F'(\eta)$ increases as M increases in the range $0 \le \eta \le 0.3$ and $0.7 \le \eta \le 1$, and decreases between $0.3 \le \eta \le 0.7$. Whereas for $|V_1| \ge |V_2|$, Figure (6) displays an opposite trend for increasing M. For $|V_2| \ge |V_1|$, Figure (4) shows the influence of β on $F'(\eta)$. It is observed that the rise in β causes a decrement in $F'(\eta)$ for $0 \le \eta \le 0.55$ and increases after 0.55 till 1. It is observed that the velocity profile shows an opposite trend for $|V_1| \ge |V_2|$ as in Figure (7).

The impact of R_2 on the temporal profile is portrayed in Figure (8). Rise in R_2 decreases $\theta(\eta)$ in the entire domain, that is, in the range $0 \leq \eta \leq 1$. Figure (9) displays the effect of M on the temporal distribution of the fluid flow. It is observed that $\theta(\eta)$ declines as M increases in the range $0 \leq \eta \leq 1$. Figure (10) depicts the impact of β on the temporal distribution. An increase in β causes a decrease in $\theta(\eta)$ for $0 \leq \eta \leq 1$. Figure (11) exhibits the impact of the Rd on the temperature curve. It is clear that an increase in Rd causes a decrease in $\theta(\eta)$. The impact of the Pr on the temperature field is displayed in Figure (12). It is observed that an increase in $\theta(\eta)$ is indicated by an increase in Pr. Figure (13) displays the impact of Eckert number on the temporal curve where an increase in Ec causes an increase in $\theta(\eta)$.

For $|V_1| \geq |V_2|$, increasing the R_1 resulted in increasing $\theta(\eta)$ as displayed in Figure(14). Figure (15) exhibits the influence of the M on the temperature curve. It is clear that an increase in M causes a decrease in $\theta(\eta)$. The impact of β on the temporal field is displayed in Figure (16). It is observed that a decrease in $\theta(\eta)$ is indicated by an increase in β. Figure (17) displays the effect of Rd on the temporal curve where an increase in Rd causes an increase in $\theta(\eta)$. It is evident from Figure (18) that an increase in Pr causes a decrease in $\theta(\eta)$. The impact of Ec on the temperature field is displayed in Figure (19). It is evident that an increase in Ec is accompanied by an increase in $\theta(\eta)$.

It is evident from Tables (1 and 2), increasing the R_i causes a decrease in the magnitude of skin friction at the bottom plate and an increase at the top plate $|V_2| \geq |V_1|$, the same trend is observed for $|V_1| \geq |V_2|$ also. It is also evident that an increment in magnetic parameter and radiation parameter is accompanied by an increase in magnitude at both plates.
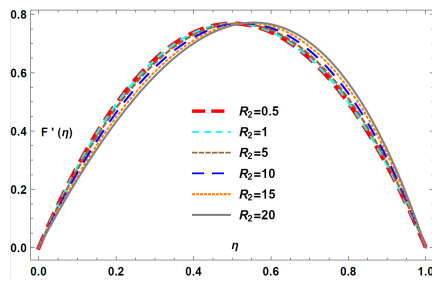

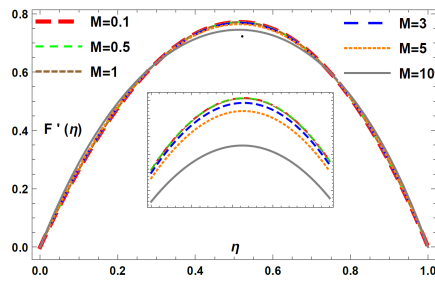FIGURE 2. Velocity profile for different R_2 when $a_2 = 0.51425, M = 3, \beta = 0.1$

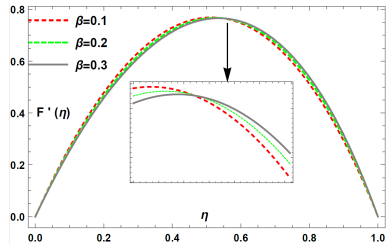FIGURE 3. Velocity profile for different M when $a_2 = 0.51425, R_2 = 5, \beta = 0.1$

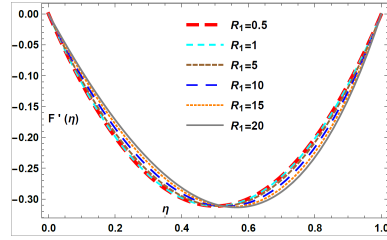FIGURE 4. Velocity profile for different β when $a_2 = 0.51425, R_2 = 5, M = 3$

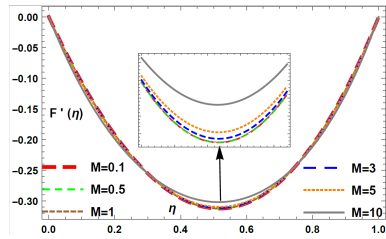FIGURE 5. Velocity profile for different R_1 when $a_1 = -0.20820, M = 3, \beta = 0.1$

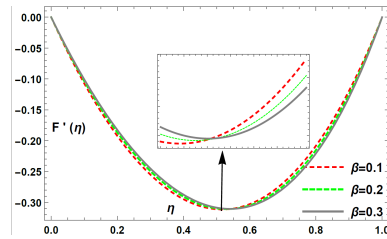FIGURE 6. Velocity profile for different M when $a_1 = -0.20820, R_1 = 5, \beta = 0.1$

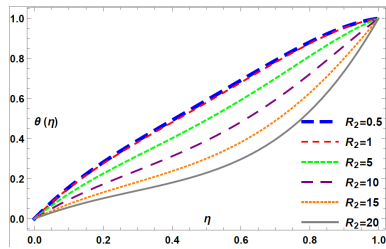FIGURE 7. Velocity profile for different β when $a_1 = -0.20820, R_1 = 5, M = 1$

FIGURE 8. Temperature profile for different R_2 when $a_2 = 0.51425, Rd = 0.2, \beta = 0.1, Pr = 0.3, M = 3, Ec = 0.2$
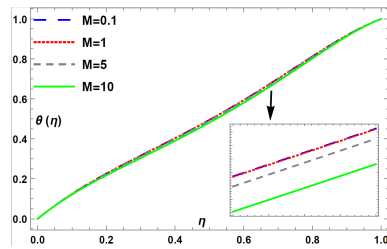

FIGURE 9. Temperature profile for different M when $a_2 = 0.51425, Rd = 0.2, Pr = 0.3, \beta = 0.1, R = 5, Ec = 0.2$
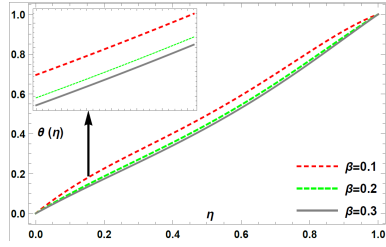
144

FIGURE 10. Temperature profile for different β when $a_2 = 0.51425, Rd = 0.2, Pr = 0.3, R_2 = 5, M = 3, Ec = 0.2$
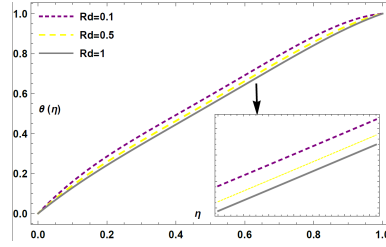

FIGURE 11. Temperature profile for different Rd when $a_2 = 0.51425, R_2 = 1, \beta = 0.1, Pr = 0.3, M = 1, Ec = 0.2$
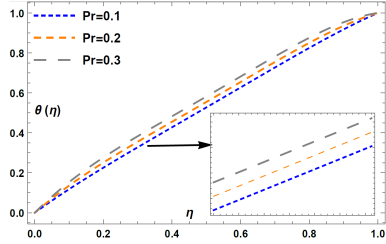

FIGURE 12. Temperature profile for different Pr when $a_2 = 0.51425, Rd = 0.2, R_2 = 1, \beta = 0.1, M = 1, Ec = 0.2$
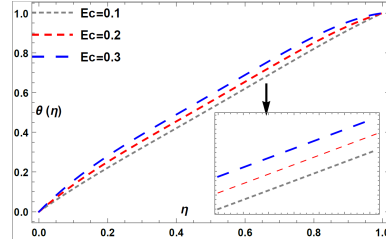

FIGURE 13. Temperature profile for different Ec when $a_2 = 0.51425, Rd = 0.2, \beta = 0.1, Pr = 0.3, M = 1, R_2 = 1$
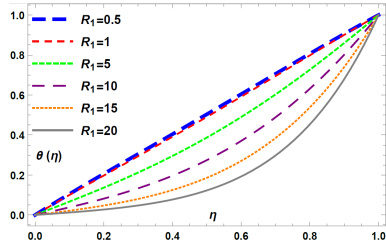

FIGURE 14. Temperature profile for different R_1 when $a_1 = -0.20820, Rd = 0.2, \beta = 0.1, Pr = 0.3, M = 3, Ec = 0.2$
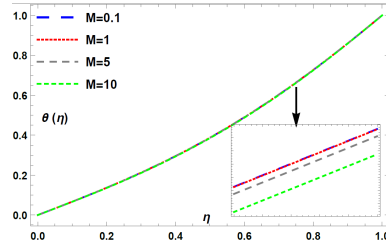

FIGURE 15. Temperature profile for different M when $a_1 = -0.20820, Rd = 0.2, Pr = 0.3, \beta = 0.1, R_1 = 5, Ec = 0.2$
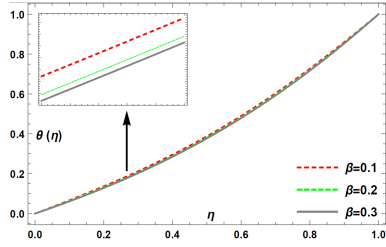
145

FIGURE 16. Temperature profile for different β when $a_1 = -0.20820, Rd = 0.2, Pr = 0.3, R_1 = 5, M = 3, Ec = 0.2$
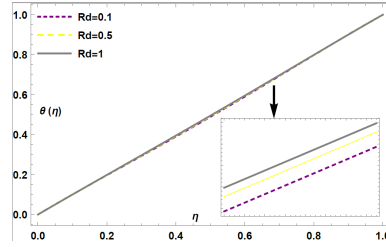

FIGURE 17. Temperature profile for different Rd when $a_1 = -0.20820, R_1 = 1, \beta = 0.1, Pr = 0.3, M = 1, Ec = 0.2$
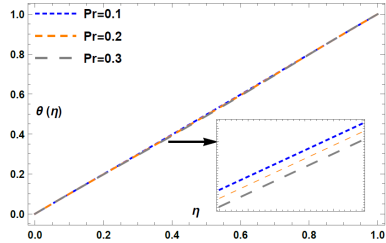

FIGURE 18. Temperature profile for different Pr when $a_1 = -0.20820, Rd = 0.2, R_1 = 1, \beta = 0.1, Ec = 0.2, M = 1$
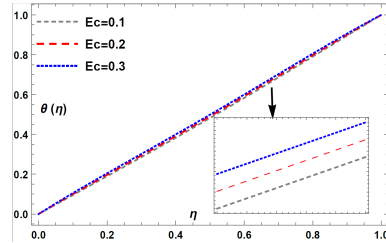
FIGURE 19. Temperature profile for different Ec when $a_1 = -0.20820, Rd = 0.2, \beta = 0.1, Pr = 0.3, M = 1, R_1 = 1$.

TABLE 1. Skin friction coefficients

R	β	$M = 0.1$			
		$a_1 = -0.20820$		$a_2 = 0.51425$	
		$F''(0)$	$F''(1)$	$F''(0)$	$F''(1)$
1	0.1	-1.23225	1.26613	3.05199	-3.12164
5		-1.16747	1.33613	2.92070	-3.27268
10		-1.09335	1.42886	2.76342	-3.47690
1	0.3	-1.20678	1.29263	3.00101	-3.17852
5		-1.05652	1.48113	2.68207	-3.59419
10		-0.90946	1.74769	2.33008	-4.21724
R	β	$M = 3$			
1	0.1	-1.24938	1.28280	3.09430	-3.16302
5		-1.18534	1.35178	2.96504	-3.31224
10		-1.11192	1.44307	2.81009	-3.51371
1	0.3	-1.25060	1.33367	3.10939	-3.28107
5		-1.10385	1.51507	2.80200	-3.68303
10		-0.95818	1.77101	2.46085	-4.28124

TABLE 2. Heat transfer rate for $M = 0.5, Ec = 0.1, Pr = 0.3$

R	β	$Rd = 0.1$			
		$a_1 = -0.2082$		$a_2 = 0.51425$	
		$\theta'(0)$	$\theta'(1)$	$\theta'(0)$	$\theta'(1)$
1	0.1	0.95407	1.03902	1.36967	0.63753
5		0.56921	1.57560	1.04259	1.12699
10		0.28698	2.39020	0.73125	1.94074
1	0.3	0.90939	1.08590	1.09318	0.92509
5		0.52872	1.62755	0.78328	1.44052
10		0.24565	2.45399	0.49695	2.27169
R	β	$Rd = 0.3$			
1	0.1	0.96233	1.03121	1.29982	0.70783
5		0.63387	1.45290	1.03091	1.09453
10		0.35802	2.08289	0.75948	1.71124
1	0.3	0.925953	1.06902	1.07547	0.939414
5		0.60013	1.49424	0.81834	1.34230
10		0.32748	2.13096	0.56511	1.96777

5. Conclusion

The current study emphasises on the Casson fluid flow between parallel plates of different permeability considering influence of applied magnetic field and thermal radiation theoretically. HPM is employed to obtain results for distinct values of the physical parameters involved. The following can be inferred from the results obtained:

- The velocity curve for mixed suction and mixed injection show opposite trend with increase M, β and R.
- The temperature profile is found to be declining as the parameters R, M and β increase in both mixed injection and mixed suction, whereas increases for increase in Eckert number.
- The temporal distribution for mixed suction and mixed injection show opposite behaviour with increase in Rd and Pr.
- The magnitude of coefficient of skin friction enhances with increasing M at both the plates.
- The magnitude of heat transmission rate enhances with increasing Rd at the lower plate, whereas declines at the top plate.
- The numerical values for rate of heat transfer are found to decay with increasing β at the lower plate, whereas rising at the top plate.
- The values of the skin friction coefficient and heat transfer decays with rising R at the lower plate, whereas enhances at the top plate.

References

1. Attia, H.A. and Kotb, N.A.: MHD flow between two parallel plates with heat transfer, in: *Acta Mechanica*, **117** (1996) 215–220.
2. Babolian, E., Azizi, A. and Saeidian, J.: Some notes on using the homotopy perturbation method for solving time-dependent differential equations, in: Mathematical and computer modelling **50(1-2)** (2009) 213–224.

3. Berman, A. S.: Laminar Flow in Channels with Porous Walls, in: *Journal of Applied Physics* **24(9)** (1953) 1232–1235.

4. Bujurke, N.M., Pai, N.P. and Achar, P.K.: Semi analytical approach to stagnation-point flow between porous plates with mass transfer, in: *Indian J. Pure appl. Math* **26(4)** (1995) 373–389.

5. Bujurke, N.M., Madalli, V.S. and Mulimani, B.G.: Long series analysis of laminar flow through parallel and uniformly porous walls of different permeability, in: *Computer methods in applied mechanics and engineering*, **160(1-2)** (1998) 39–56.

6. Ganesh, S. and Krishnambal, S.: Magnetohydrodynamic flow of viscous fluid between two parallel porous plates,in: *Journal of Applied sciences* **6(11)** (2006) 2420–2425.

7. Ganesh, S., Babu, R. Delhi, Anand, V. W. J. and Chandrasekar, P.: Magnetohydrodynamic flow of viscous fluid between two parallel porous plates with bottom injection and top suction, in: *International Journal of Ambient Energy*, **42(4)** (2021) 393–396.

8. Gupta, S., Kumar, D., and Singh., J.: Application of he's homotopy perturbation method for solving nonlinear wave-like equations with variable coefficients, in: *International Journal of Advances in Applied Mathematics and Mechanics* **1(2)** (2013) 65–79.

9. Hamza E.A.: Suction and injection impacts on a similar flow between parallel plates, in: *Journal of Physics D: Applied Physics* **32(6)** (1999) 656–663.

10. Hayat, T., Saif, R. S., Abbas, Z., Sajid, M. and Hendi, A.: Radiation impacts on MHD flow of Maxwell fluid in a channel with porous medium, in: *International Journal of Heat and Mass Transfer* **54(4)** (2011) 854–862.

11. He, J. H.: Homotopy perturbation technique, in: *Computer Methods in Applied Mechanics and Engineering* **178(3)** (1999) 257–262.

12. He, J. H.: Homotopy perturbation method: a new nonlinear analytical technique, in: *Applied Mathematics and Computation* **135(1)** (2003) 73–79.

13. Makinde, O.D.: Free convection flow with thermal radiation and mass transfer past a moving vertical porous plate, in: *International Communications in Heat and Mass Transfer*, **32(10)** (2005) 1411–1419.

14. Mukhopadhyay, S., Layek, G.C.: Radiation impact on forced convective flow and heat transfer over a porous plate in a porous medium, in: *Meccanica* **44** (2009) 587–597.

15. Naduvinamani, N.B. and Shankar, U.: Radiative squeezing flow of unsteady magnetohydrodynamic Casson fluid between two parallel plates, in; *Journal of Central South University* **26(5)** (2019) 1184–1204.

16. Raptis, A.: Radiation and free convection flow through a porous medium, in: *International Communications in Heat and Mass Transfer* **25(2)** (1998) 289–295.

17. Saberi-Nadjafi, J. and Zahmatkesh, S.: Homotopy perturbation method (HPM) for solving higher order boundary value problems (BVP), in: *Appl Math Comput Sci* **1(2)** (2010) 199–224.

18. Sachdev, P. L., Bujurke, N. M. and Pai, N. P.: Dirichlet series solution of equations arising in boundary layer theory, in: *Mathematical and Computer Modelling* **32(9)** (2000) 971–980.

19. Sampath Kumar, V.S. and Pai, N. P.: Suction and injection impact on flow between two plates with reference to Casson fluid model, in: *Multidiscipline Modeling in Materials and Structures* **15(3)** (2018) 559–574.

20. Sampath Kumar, V.S. and Pai, N. P. and Jacub, K.: A semi-numerical approach to unsteady squeezing flow of casson fluid between two parallel plates, in: *Malaysian Journal of Mathematical Sciences* **12(1)** (2018) 35–47.

21. Sampath Kumar, V.S., Pai,N. P., and Devaki, B.: Analysis of MHD flow and heat transfer of laminar flow between porous disks, in: *Frontiers in Heat and Mass Transfer (FHMT)* **16(3)** (2021) 1–9.

22. Sellars, John R.: Laminar flow in channels with porous walls at high suction Reynolds numbers, in: *Journal of Applied Physics* **26(4)** (1955) 489–490.

23. Sithole,H., Mondal, H., Goqo, S., Sibanda, P. and Motsa, S.: Numerical simulation of couple stress nanofluid flow in magneto-porous medium with thermal radiation and a chemical reaction, in: *Applied Mathematics and Computation* **339** (2018) 820–836

24. Srinivas, S., Kumar, C. K. and Reddy, A. S.: Pulsating flow of Casson fluid in a porous channel with thermal radiation, chemical reaction and applied magnetic field, in: *Nonlinear Analysis: Modelling and Control* **23(2)** (2018) 213–233. year=2018

25. Terrill, Robert M.: Laminar flow in a uniformly porous channel, in: *Aeronautical Quarterly* **15(3)** (1964) 299–310.

26. Terrill, Robert M. and Shrestha, Gambhir M.: Laminar flow through parallel and uniformly porous walls of different permeability, in: *Journal of Applied Mathematics and Physics (ZAMP)* **16** (1965) 470–482.

27. Yuan, S.W.: Further investigation of laminar flow in channels with porous walls, in: *Journal of Applied physics* **27(3)** (1956) 267–269.

Nityanand P. Pai: Department of Mathematics, Manipal Institute of Technology, Manipal Academy of Higher Education, Manipal, Karnataka 576104, India
Email address: nppaimit@yahoo.co.in

Devaki B.: Department of Mathematics, Manipal Institute of Technology, Manipal Academy of Higher Education, Manipal, Karnataka 576104, India
Email address: devakibadekkila@gmail.com

Pareekshith: Department of Mathematics, Manipal Institute of Technology, Manipal Academy of Higher Education, Manipal, Karnataka 576104, India
Email address: pareekshithgb@gmail.com

Sampath Kumar V. S.: Department of Mathematics, Manipal Institute of Technology, Manipal Academy of Higher Education, Manipal, Karnataka 576104, India
Email address: sampathkmr322@gmail.com * Corresponding author

Vasanth K. R.: Department of Mathematics, NMAM Institute of Technology (Nitte deemed to be University), Nitte, Karnataka 574110, India
Email address: drvasanth@nitte.edu.in